



## Enhanced carbide precipitation during tempering of sub-zero Celsius treated AISI 52100 bearing steel

Villa, Matteo; Pantleon, Karen; Somers, Marcel A. J.

*Publication date:*  
2013

*Document Version*  
Peer reviewed version

[Link back to DTU Orbit](#)

*Citation (APA):*

Villa, M., Pantleon, K., & Somers, M. A. J. (2013). *Enhanced carbide precipitation during tempering of sub-zero Celsius treated AISI 52100 bearing steel*. Paper presented at Heat Treat & Surface Engineering Conference & Expo 2013, Chennai, India.

---

### General rights

Copyright and moral rights for the publications made accessible in the public portal are retained by the authors and/or other copyright owners and it is a condition of accessing publications that users recognise and abide by the legal requirements associated with these rights.

- Users may download and print one copy of any publication from the public portal for the purpose of private study or research.
- You may not further distribute the material or use it for any profit-making activity or commercial gain
- You may freely distribute the URL identifying the publication in the public portal

If you believe that this document breaches copyright please contact us providing details, and we will remove access to the work immediately and investigate your claim.

# Enhanced carbide precipitation during tempering of sub-zero Celsius treated AISI 52100 bearing steel

Matteo Villa, Karen Pantleon, Marcel A.J. Somers

Technical University of Denmark, Department of Mechanical Engineering  
DK 2800 Kongens Lyngby, Denmark

[matv@mek.dtu.dk](mailto:matv@mek.dtu.dk), [kapa@mek.dtu.dk](mailto:kapa@mek.dtu.dk), [somers@mek.dtu.dk](mailto:somers@mek.dtu.dk)

**Keywords:** martensite, tempering, sub-zero Celsius treatment, (synchrotron) XRD, dilatometry

**Abstract.** A 1.5%Cr, 1%C bearing steel was sub-zero Celsius treated after quenching. Transmission and reflection (synchrotron) X-Ray Diffraction were applied ex-situ at the HZB-BESSY II synchrotron facility to quantify the phase fractions of martensite and austenite and determine the stress state in austenite.

The tempering response of the sub-zero treated material was studied with high resolution dilatometry and compared with the behavior of a reference as-quenched sample. X-Ray Diffraction indicates that sub-zero Celsius treating reduces the content of retained austenite in the material and introduces a state of compression in austenite. Dilatometry indicates that a long isothermal holding at cryogenic temperatures enhanced the precipitation of transition carbides during tempering.

## Introduction

High carbon steels are used for bearings, cutting tools, dies and more generally applications that require mechanical stability, high hardness and wear resistance.

As an additional step in quenching and tempering heat treatment, sub-zero Celsius treating may improve the performance of high carbon steels, particularly with regard to wear resistance [1–6]. This improvement is of particular technological interest, since it drives to noteworthy economical savings enhancing life service of steel products.

The metallurgical mechanisms that cause enhanced wear resistance are not fully understood yet. Reviews on the topic [7–11] put forward the following interpretations: (i) a reduction of the content of retained austenite; (ii) an enhanced and more uniform precipitation of transition carbides; (iii) a modification of the sub-structure of martensite; (iv) a more favorable macro-stress state.

Among these possibilities, observations in [6,11–14] support enhanced and more uniform precipitation as the key point. However, the mechanism responsible for the modification of the precipitation process is not clarified.

It is documented that, both wear resistance and precipitation of carbides are promoted by an isothermal, i.e. thermally activated, process occurring at cryogenic temperatures (lower than  $-80^{\circ}\text{C}$ ) [3,15–18].

The following interpretations for the thermally activated process have been put forward [7–11]: (i) diffusion of carbon atoms to nearby lattice defects, resulting in the formation of carbon clusters that may act as nucleation sites for the precipitation of carbides, is an interpretation that appears inconsistent with the availability of thermal energy for the diffusion of carbon atoms in iron, insufficient at temperatures below  $-50^{\circ}\text{C}$  [19–21]; (ii) modification of the martensite sub-structure and stress state (martensite conditioning) during isothermal holding at cryogenic temperatures, is an interpretation that remains phenomenological; (iii) modified tetragonality of martensite upon sub-zero Celsius treating [22–24] is a phenomenon that does not require isothermal holding, hence it is an interpretation that does not appear consistent; (iv) thermally activated martensite formation.

Martensite formation occurs in connection with a noteworthy transformation strain and may introduce lattice defects and a new state of stress in the material [24,25]. Also it can assist the formation of carbon clusters [19].

Thermally activated martensite formation was first reported in [26] and is reviewed in [27]. In 1%C, 1.5%Cr bearing steels, thermally activated martensite formation was reported in [24,28–29], and is a particularly relevant phenomenon at cryogenic temperatures.

In [24], it was suggested that below a critical temperature (about  $-140^{\circ}\text{C}$ ), the transformation strain associated with martensite formation is accommodated in the existing martensite and generates nucleation sites for the precipitation of transition carbides during tempering.

This paper seeks to investigate the effect of a long isothermal holding at cryogenic temperature on the precipitation of transition carbides during tempering and aims to contribute to the understanding of the thermally activated process responsible for enhanced and more uniform precipitation.

## Experimental

**Material and sample geometries.** The alloy investigated is a commercial AISI 52100 steel with the composition given in Table 1 and extruded to a 10mm rod. For dilatometry 10 mm high hollow cylinders were prepared with outer and inner diameter of  $\varnothing 4.0$  and  $\varnothing 3.6$ , respectively; for (synchrotron) X-Ray Diffraction (XRD)  $\varnothing 3\text{mm}$ , 0.2mm thick disks were prepared.

*Table 1: Chemical composition (in wt-%) of AISI 52100 as determined by Glow Discharge Optical Emission Spectrometry (GDOES)*

Fe	C	Cr	Ni	Mn	Si	Mo	Cu
Bal.	$0.96 \pm 0.02$	$1.60 \pm 0.05$	$0.10 \pm 0.01$	$0.28 \pm 0.04$	$0.13 \pm 0.04$	$0.05 \pm 0.01$	$0.15 \pm 0.01$

**Heat treatments.** The applied heat treatments are schematically reported in Fig. 1. Austenitization (Fig. 1a) was performed at  $1080^{\circ}\text{C}$  for 60s, followed by a quench in oil at  $140^{\circ}\text{C}$ ; the material was kept in the oil bath for 20 s and air cooled before storage at room temperature for about 2 Ms (3-4 weeks). Protection from oxidation during austenitization was ensured through embedding the samples in 4 layers of  $30\ \mu\text{m}$  thick foils of stainless steel AISI 316.

Three different thermal cycles were performed after austenitization and 2 Ms storage (Fig. 1b): “AsQ” refers to samples not subjected to any sub-zero Celsius treatment, but stored further 2 Ms at room temperature; “C” refers to samples cooled at  $15\ \text{K}/\text{min}$  to  $-150^{\circ}\text{C}$  and thereafter (re)heated at  $15\ \text{K}/\text{min}$  to room temperature before a second storage period of 2 Ms at room temperature; “C+H” refers to samples that were cooled at  $15\ \text{K}/\text{min}$  to  $-150^{\circ}\text{C}$ , held 72h at  $-150^{\circ}\text{C}$ , (re)heated at  $15\ \text{K}/\text{min}$  to  $-110^{\circ}\text{C}$ , held 24h at  $-110^{\circ}\text{C}$  and finally (re)heated at  $15\ \text{K}/\text{min}$  to room temperature before a second storage period of 2 Ms at room temperature. In the sequel samples are referred to as “starting” condition AsQ, C and C+H, depending on the performed thermal cycle. For the samples in the starting conditions, the total storage time at room temperature after initial quenching is about 4 Ms.

The material in the three different starting conditions was thereafter subjected to tempering. The tempering (Fig. 1c) of martensite was followed with dilatometry during isochronal heating of the material at  $1.5\ \text{K}/\text{min}$  up to  $350^{\circ}\text{C}$ . XRD was applied at room temperature on samples heated at  $1.5\ \text{K}/\text{min}$  to  $180^{\circ}\text{C}$  only and air cooled.

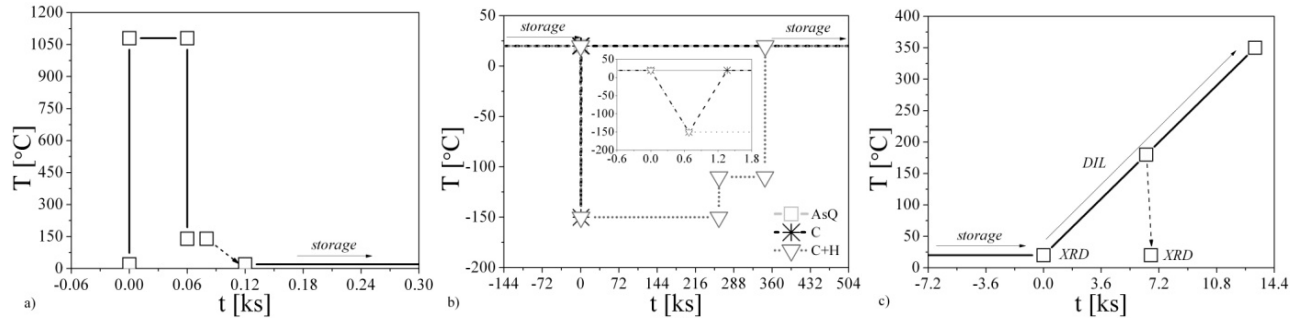


Figure 1. Heat treatments: a) austenitization; b) sub-zero Celsius treatments; c) tempering.

**Methods.** XRD was performed at the synchrotron facility HZB-BESSY II at the experimental station EDDI [30]. XRD investigation was performed prior to tempering and after heating at 1.5K/min to 180°C (Fig. 1c). These measurements were performed at room temperature in transmission geometry and averaged over the whole samples thickness. Details on the measurement conditions, the quantitative phase analysis and the determination of the lattice parameter of austenite are reported in [24]. The stress state in austenite was evaluated in reflection geometry applying the  $\sin^2\psi$  method [31]; experimental details were reported in [25]. Dilatometry was performed in a Bähr DIL 805A/D dilatometer. The length change of the samples was measured during isochronal heating at 1.5K/min up to 350°C (Fig.1c).

## Results

**X-Ray Diffraction, XRD.** The results of the (synchrotron) XRD investigations prior to the tempering step and after isochronal heating at 1.5K/min to 180°C are reported in Table 2.

Table 2: Results of the XRD investigations: content of retained austenite,  $f_\gamma$ ; lattice parameter of austenite,  $a_\gamma$ , probed for the  $(h k l)$  200, 220, 311 and 420 reflections; tetragonality of martensite expressed as the ratio between the crystallographic axes  $c$  and  $a$ ,  $c/a$  ratio; macro-stresses in austenite reported in terms of  $\sigma_{\parallel} - \sigma_{\perp}$  (average and standard deviation for probed 200, 220, 311 and 420 reflections), where  $\parallel$  is a general direction parallel to the sample surface and  $\perp$  is the surface normal.

Starting condition	$f_\gamma$ [%]	Treatment	c/a ratio	$a_\gamma$ [Å]				$\sigma_{\parallel} - \sigma_{\perp}$ [MPa]
				200	220	311	420	
AsQ	29.2	Prior tempering	1.036	3.606	3.602	3.604	3.605	5±24
		After heating	≈1	3.607	3.598	3.599	3.599	-23±9
C	11.9	Prior tempering	1.037	3.604	3.597	3.599	3.601	23±29
		After heating	≈1	3.608	3.598	3.598	3.599	-48±29
C+H	7.7	Prior tempering	1.036	3.600	3.595	3.598	3.600	3±9
		After heating	≈1	3.608	3.594	3.597	3.594	-71±23

The XRD investigations show that both the applied sub-zero Celsius treatments reduce the content of retained austenite in the material. As follows from the last column in Table 2, the difference in in-plane and normal macro-stress components in austenite is nil within experimental accuracy. Comparing the lattice parameters determined for the various  $hkl$  of austenite in the three samples prior to tempering shows clearly that austenite is in a compressed state of stress after sub-zero Celsius treatment. Hence, with  $\sigma_{\parallel} - \sigma_{\perp} \approx 0$  austenite experiences a state of hydrostatic compression, most specifically for C+H. Locally, strains appear concentrated along specific crystallographic directions (the measured lattice parameter of austenite depends on the probed reflection). The tetragonality of martensite does not depend on the starting condition.

During heating to 180°C, martensite loses its tetragonality. The stress state in austenite is (mainly) hydrostatic, albeit with a slight net compression in the plane of the sample disc. Evidently, the local strain direction is observed to change during heating and to depend on the starting condition.

**Dilatometry (DIL).** The results of dilatometry investigations are reported in Fig. 2: the linear thermal expansion coefficient at the beginning of the tempering step is given in Fig. 2a, while Fig. 2b shows the contraction/expansion of the samples during solid state transformation.

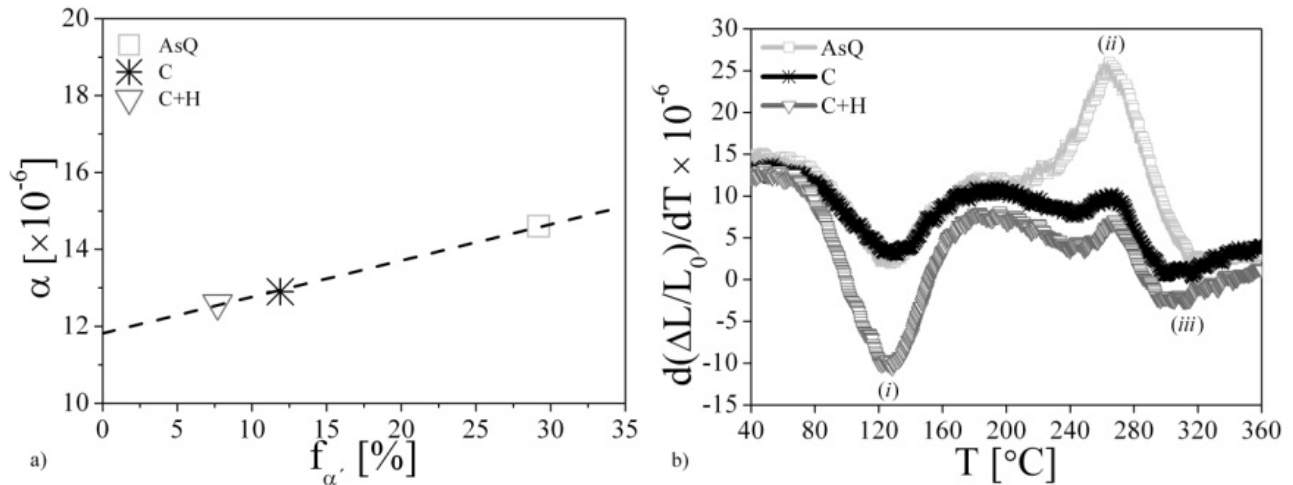


Figure 2. a) linear thermal expansion coefficients  $\alpha$  measured in the temperature interval 40-50°C during isochronal heating at 1.5K/min. b) differentiated relative sample elongation,  $d(\Delta L/L_0)/dT$ , vs. temperature,  $T$ , during isochronal heating.

Fig. 2a shows that the linear thermal expansion coefficient scales with the variation in austenite fraction. In Fig. 2b three phase transitions are discerned, indicated by (i), (ii) and (iii). Transition (i) is most pronounced for the sample subjected to C+H treatment, while peak (ii) is largest for sample AsQ. No clear differences can be observed for peak (iii).

## Interpretation

**X-Ray Diffraction.** As expected sub-zero Celsius treatment reduces the amount of retained austenite in AISI 52100. The observation of a lower content of retained austenite for condition C+H as compared to condition C indicates that isothermal treatment is an important step in the treatment. During the long isothermal cryogenic treatment thermally activated martensite formation occurs. In-situ observation and investigation of thermally activated martensite formation for the present AISI 52100 is reported elsewhere and shows that mainly thermally activated growth of martensite nuclei, developed during cooling, into lenticular martensite occurs [24,32].

Martensite formation introduces a (macroscopically hydrostatic) state of compression in austenite that depends locally (microscopically) on the probed crystallographic direction [25]. It has been suggested that the compression is concentrated along the shape strain direction [25] and results from a partial elastic accommodation of the transformation strain in austenite. The compression is the larger, the more martensite forms [29]. In the present study, the introduction of (additional) compressive stress in austenite as observed between the starting condition AsQ and the condition C and C+H is directly ascribed to martensite formation. Also, the observation of a larger compression for the starting condition C+H as compared to the starting condition C is ascribed to the larger amount of transformation occurring in C+H.

Concerning martensite tetragonality, at temperatures above about  $-40^{\circ}\text{C}$ , the availability of thermal energy is sufficient for the movement of carbon atoms of short distances [19–21] in iron and the tetragonal cell of martensite can relax [33–36]. At room temperature, relaxation is close to

saturation after about 0.2 Ms [36]. The apparent insensitivity of martensite tetragonality on the starting condition as observed in the present study is ascribed to saturation of the relaxation phenomena during long time storage at room temperature ( $> 2$  Ms).

For 1.5K/min heating rates, the crystal lattice of martensite becomes cubic in the temperature interval 90–140°C, as a consequence of the precipitation of transition carbides [24,37,38]. Data in the present study shows that the unit cell of martensite does not show any tetragonality upon heating to 180°C where precipitation of transition carbides is finished (cf. peak (i) in Fig. 2b). The present investigation does not allow definitive conclusions on the stress state of the material after heating to 180°C due to the fact that carbon atoms may have diffused enriching or depleting the different phases (modifying their lattice parameters). Moreover, carbon redistribution is known to be influenced by sub-zero treating for the present system [24]. On the other hand, the strain (re)distribution between different probed crystallographic directions cannot be appointed to carbon redistribution between phases.

Transition carbides precipitate in association with a volumetric contraction of the material and a defined orientation relationship with the parent martensite phase [39–41]; also, it was suggested that a modification in the martensite sub-structure may alter the orientation relationship [42]. Data in the present study suggests that the precipitation of transition carbides has altered the local stress state in the material in a systematic way. The macroscopic state of stress in austenite,  $\sigma_{\parallel} - \sigma_{\perp}$ , has changed to a net compressive stress within the plane of the sample. Further, additional elastic strains are introduced along specific crystallographic directions of austenite (that is related to martensite with an orientation relationship). The observation of a quantitative difference between starting conditions C and C+H for the 220 and 420 probed reflections may indicate either a difference in the amount of precipitation, a different precipitation mechanism, or a combination of both.

**Dilatometry.** As a consequence of the closer packing of the f.c.c. lattice than the b.c.t. lattice, the linear thermal expansion of austenite is larger than the linear thermal expansion of martensite. The linear proportionality of the linear expansion coefficient with the austenite content in Fig. 2b is consistent with this expectation. Extrapolation to pure martensite and pure austenite gives  $11.9 \cdot 10^{-6} \text{ K}^{-1}$  and  $21.3 \cdot 10^{-6} \text{ K}^{-1}$ , respectively. These values are in reasonable agreement with literature values of  $10.9 \cdot 10^{-6} \text{ K}^{-1}$  and  $23.4 \cdot 10^{-6} \text{ K}^{-1}$  [29], respectively.

The transformation peaks in Fig. 2b are interpreted on the basis of the analysis in [35,43].

According to [35,43], precipitation of secondary transition carbides (peak (i)) and formation of cementite (peak (iii)) are associated with volume reductions, while decomposition of retained austenite (peak (ii)) induces a volume expansion. From Fig. 2b, a significant reduction of the retained austenite content in cryogenic treated samples is demonstrated: peak (ii) is largely reduced for sample C and C+H as compared to sample AsQ.

Interestingly, peak (i) is equivalent for starting conditions C and AsQ, but differs spectacularly for sample C+H. Dilatometry results show that enhanced precipitation of transition carbides (peak (i)) is promoted only by long isothermal holding at cryogenic temperatures, while no effects are reported for (controlled) sub-zero Celsius cooling to the same cryogenic temperature.

## Discussion

The present study strongly supports the notion that enhanced precipitation of transition carbides during tempering can be ascribed to a thermally activated process in the isothermal stage during sub-zero Celsius treatment.

Among the interpretations listed in the introduction section, the present experimental data exclude the tetragonality of martensite as a key parameter in governing enhanced precipitation during tempering.

Further investigation, including in-situ investigation and direct observation of the precipitation products is necessary to definitively establish the nature of the thermally activated process.

On the basis of previous experimental activity by the present authors [24], enhanced precipitation is hereby interpreted as a consequence of thermally activated martensite formation at cryogenic temperatures that conditions existing martensite and generates new nucleation sites for the carbides precipitates during tempering.

This interpretation suggests that the investigation of the effects of sub-zero Celsius treatments should be driven towards the theory of the martensitic transformation in steel.

## Conclusions

Sub-zero Celsius treatments are effective in reducing the content of retained austenite in high carbon steels.

The main microstructural difference between a simple sub-zero Celsius cooling and a sub-zero Celsius cooling followed by a long isothermal holding at cryogenic temperature, analyzed before tempering, is a further reduction of the amount of retained austenite. No effect of cryogenic treatment is observed on the tetragonality of martensite.

Sub-zero Celsius cooling alone is not effective in promoting enhanced precipitation of transition carbides. The present work demonstrates that enhanced precipitation can be obtained during tempering after a long isothermal holding at cryogenic temperatures. In the isothermal stage thermally activated martensite develops.

## Acknowledgements

The authors are indebted Mikkel F. Hansen from the Technical University of Denmark for the controlled sub-zero Celsius treatments. M. Reich, University of Rostock, is gratefully acknowledged for performing the dilatometry experiments. The authors acknowledge the Danish Natural Science Research Council for financial support of the work at the Berlin synchrotron facility HZB-BESSY II via Danscatt.

## References

- [1] M.A. Jaswin, G. S. Shankar, D. Mohan Lal, *Int. J. Precision Eng. and Manuf.*, 11-1 (2010) 97-105
- [2] D. Mohal Lal, S. Renganarayanan, A. Kalanidhi, *Cryogenics*, 41 (2001) 149-155
- [3] K. Amini, S. Nategh, A. Shafyei, *Mater. And Design*, 31 (2012) 4666-4675
- [4] R.F. Barron, *Cryogenics*, 22 (1982) 409-413
- [5] D. Das, A. K. Dutta, K.K. Ray, *Mat. Sci. Eng. A*, 527 (2010) 2182-2193
- [6] F. Meng, K. Tagashira, H. Sohma, *Scripta Mater*, 31:7 (1994) 865-868
- [7] S.S. Gill, H. Singh, R. Singh, J. Singh, *Int. J. Adv. Manuf. Technol.*, 48 (2010) 175-192
- [8] S.S. Gill, J. Singh, R. Singh, H. Singh, *Int. J. Adv. Manuf. Technol.*, 54 (2011) 59-82
- [9] W. Reitz, J. Pendray, *Mater. Manuf. Processes*, 16:6 (2001) 829-840
- [10] D. N. Collins, *Heat treatment of Metals*, 3 (1997) 71
- [11] D. Das, A.K. Dutta, K.K. Ray, *Mat. Sci. Eng., A* 527 (2010) 2182-2193
- [12] F. Meng, K. Tagashira, R. Azuma, H. Sohma, *ISIJ Int.*, 34 (1994) 205-210
- [13] P.F. Stratton, *Mat. Sci. Eng., A* 449-451 (2007) 809-812
- [14] J.Y. Huang, Y.T. Zhu, X.Z. Liao, I.J. Beyerlein, M.A. Bourke, T.E. Mitchell, *Mat. Sci. Eng. A*, 339 (2003) 241-244
- [15] D. Mohal Lal, S. Renganarayanan, A. Kalanidhi, *Cryogenics*, 41 (2001) 149-155
- [16] D. Das, A.K. Dutta, K.K. Ray, *Wear* 266 (2009) 297-309
- [17] D. Das, A.K. Dutta, K.K. Ray, *Phil. Mag.*, 89 1 (2009) 55-76
- [18] D.N. Collins, J. Dormer, *Heat Treat. Metals*, 3 (1997) 71
- [19] A.I. Tyshchenko, W. Theisen, A. Oppenkowski, S. Siebert, O.N. Razumov, A.P. Skoblik, V.A. Sirosh, Yu.N. Petrov, V.G. Gavriljuk, *Mat. Sci. Eng. A*, 527 (2010) 7027-7039

- [20] D.E Kaputkin, Mat. Sci. Eng., A 438-440 (2006) 207-211
- [21] P.C. Chen, B.O. Hall, P.G. Winchell, Metall. Trans., A 11 (1980) 1323-1331
- [22] A. Bensely, S. Venkatesh, D. Mohan Lal, G. Nagarajan, A. Rajadurai, K. Junik, Mat. Sci. Eng. A, 479 (2008) 229-235
- [23] I. Wierszyloski, J. Samolczyk, S. Wieczorek, E. Andrzejewska, A. Marcinkowska, Def. Diff. Forum, 273-276 (2008) 731-739
- [24] M. Villa, K. Pantleon, M.A.J. Somers, “*Evolution of compressive strains in retained austenite during sub-zero martensite formation and tempering*”, submitted
- [25] M. Villa, K. Pantleon and Marcel A.J. Somers, Scripta Mater. 67 (2012) 621-624
- [26] G.V. Kurdjumov, O.P. Maksimove, Dokl. Akad. Nauk SSSR, 61 (1948) 83
- [27] N.N. Thadhani, M.A. Meyers, Progress in Mater. Sci., 30 (1986) 1-37
- [28] A. Stojko, M.F. Hansen, J. Slycke, M.A.J. Somers, J. of ASTM Int., 8:4 (2011)
- [29] M. Villa, K. Pantleon, M.A.J. Somers, “*Ab-normal martensite formation during sub-zero treatment of ball bearing steel*”, submitted
- [30] Ch. Genzel, I.A. Denks, J. Gibmeier, M. Klaus, G. Wagener. Nuclear Instruments and Methods in Physics Research A, 578 (2007) 23–33
- [31] V. Hauk, Structural and Residual Stress Analysis by Non-Destructive Methods: Evaluation – Application – Assessment, Elsevier Science, Amsterdam, 1997
- [32] M. Villa, PhD thesis, in preparation
- [33] P.C. Chen, P.G. Wichell, Metall Trans., A 11 (1980) 1333-1339
- [34] A. M. Sherman, G.T. Eldis, M. Cohen, Metall. Trans., A 14 (1983) 995-1005
- [35] L. Cheng, C.M. Brakman, B.M. Korevaar, E.J. Mittemeijer, Metall. Trans., A 19 (1988) 2415-2426
- [36] L. Cheng, N.M. van der Pers, A. Bottger, Th.H. de Keijser, E.J. Mittemeijer, Metall. Trans. A 22A (1991) 1957–1967
- [37] M.J. van Genderen, M. Isac, A. Bottger, E.J. Mittemeijer, Metall. Trans., A 28 (1997) 545-561
- [38] A.T.W. Barrow, J-H. Kang, P.E.J. Rivera-Diaz-del-Castillo, Acta mater., 60 (2012) 2805-2815
- [39] M.G.H. Wells, Acta Mater, 12 (1964) 389-399
- [40] S. Nagakura, Y. Hirotsu, M. Kusunoki, T. Suzuki, Y. Nakamura, Metall. Trans., A 14 (1983) 1025-1031
- [41] H.K.D.H. Bhadeshia, Worked Examples in the Geometry of Crystals, The Institute of Metals, London, 1987
- [42] K.A. Taylor, G.B: Olson, M. Cohen, J.B. Vander Sande, Metall. Trans., A 20 (1989) 2749-2765
- [43] P.V. Morra, A.J. Böttger, E.J. Mittemeijer, J. Thermal Analysis and Calorimetry, 64 (2001) 905-914